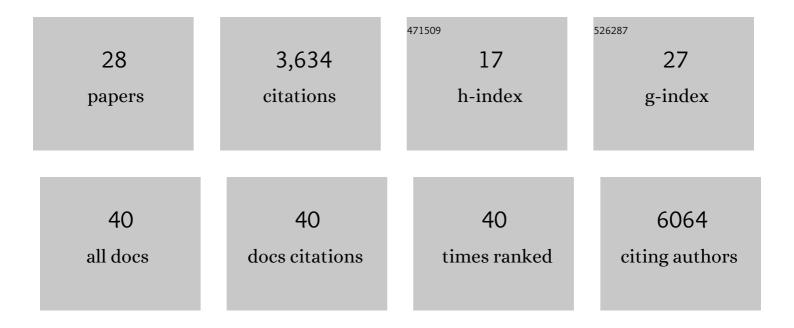
## Nels C Elde

List of Publications by Year in descending order

Source: https://exaly.com/author-pdf/2598579/publications.pdf Version: 2024-02-01



NELS C FLDE

#	Article	IF	CITATIONS
1	Regulatory activities of transposable elements: from conflicts to benefits. Nature Reviews Genetics, 2017, 18, 71-86.	16.3	1,065
2	Regulatory evolution of innate immunity through co-option of endogenous retroviruses. Science, 2016, 351, 1083-1087.	12.6	760
3	Poxviruses Deploy Genomic Accordions to Adapt Rapidly against Host Antiviral Defenses. Cell, 2012, 150, 831-841.	28.9	281
4	Protein kinase R reveals an evolutionary model for defeating viral mimicry. Nature, 2009, 457, 485-489.	27.8	250
5	cGAS-mediated stabilization of IFI16 promotes innate signaling during herpes simplex virus infection. Proceedings of the National Academy of Sciences of the United States of America, 2015, 112, E1773-81.	7.1	220
6	Escape from bacterial iron piracy through rapid evolution of transferrin. Science, 2014, 346, 1362-1366.	12.6	186
7	The evolutionary conundrum of pathogen mimicry. Nature Reviews Microbiology, 2009, 7, 787-797.	28.6	183
8	Buried Treasure: Evolutionary Perspectives on Microbial Iron Piracy. Trends in Genetics, 2015, 31, 627-636.	6.7	111
9	Wham: Identifying Structural Variants of Biological Consequence. PLoS Computational Biology, 2015, 11, e1004572.	3.2	105
10	Overlapping Patterns of Rapid Evolution in the Nucleic Acid Sensors cGAS and OAS1 Suggest a Common Mechanism of Pathogen Antagonism and Escape. PLoS Genetics, 2015, 11, e1005203.	3.5	82
11	Coevolution of Genome Architecture and Social Behavior. Trends in Ecology and Evolution, 2019, 34, 844-855.	8.7	49
12	DisAp-dependent striated fiber elongation is required to organize ciliary arrays. Journal of Cell Biology, 2014, 207, 705-715.	5.2	43
13	Recurrent Loss-of-Function Mutations Reveal Costs to OAS1 Antiviral Activity in Primates. Cell Host and Microbe, 2019, 25, 336-343.e4.	11.0	37
14	Emergence of a Viral RNA Polymerase Variant during Gene Copy Number Amplification Promotes Rapid Evolution of Vaccinia Virus. Journal of Virology, 2017, 91, .	3.4	36
15	Antimicrobial Functions of Lactoferrin Promote Genetic Conflicts in Ancient Primates and Modern Humans. PLoS Genetics, 2016, 12, e1006063.	3.5	32
16	Linking Virus Discovery to Immune Responses Visualized during Zebrafish Infections. Current Biology, 2020, 30, 2092-2103.e5.	3.9	29
17	Long read sequencing reveals poxvirus evolution through rapid homogenization of gene arrays. ELife, 2018, 7, .	6.0	23
18	Exploiting species specificity to understand the tropism of a human-specific toxin. Science Advances, 2020. 6. eaax7515.	10.3	21

Nels C Elde

#	Article	IF	CITATIONS
19	Signatures of host–pathogen evolutionary conflict reveal MISTR—A conserved MItochondrial STress Response network. PLoS Biology, 2020, 18, e3001045.	5.6	20
20	Natural rodent model of viral transmission reveals biological features of virus population dynamics. Journal of Experimental Medicine, 2022, 219, .	8.5	18
21	Baculovirus protein PK2 subverts eIF2α kinase function by mimicry of its kinase domain C-lobe. Proceedings of the National Academy of Sciences of the United States of America, 2015, 112, E4364-73.	7.1	14
22	Determinants for degradation of SAMHD1, Mus81 and induction of G 2 arrest in HIV-1 Vpr and SIVagm Vpr. Virology, 2015, 477, 10-17.	2.4	11
23	RetroCHMP3 blocks budding of enveloped viruses without blocking cytokinesis. Cell, 2021, 184, 5419-5431.e16.	28.9	8
24	Rapid Evolution of Primate Type 2 Immune Response Factors Linked to Asthma Susceptibility. Genome Biology and Evolution, 2017, 9, 1757-1765.	2.5	7
25	Diarrheal pathogens trigger rapid evolution of the guanylate cyclase-C signaling axis in bats. Cell Host and Microbe, 2021, 29, 1342-1350.e5.	11.0	5
26	Poliovirus Evolution: The Strong, Silent Type. Cell Host and Microbe, 2012, 12, 605-606.	11.0	4
27	Recurrent evolution of an inhibitor of ESCRT-dependent virus budding and LINE-1 retrotransposition in primates. Current Biology, 2022, 32, 1511-1522.e6.	3.9	2
28	Nels Elde. Current Biology, 2021, 31, R1410-R1412.	3.9	0